ACS APPLIED MATERIALS & INTERFACES

RESEARCH ARTICLE

www.acsami.org

A Self-Templated Etching Route to Surface-Rough Silica Nanoparticles for Superhydrophobic Coatings

Xin Du[†,‡] and Junhui He[†,*]

[†]Functional Nanomaterials Laboratory and Key Laboratory of Photochemical Conversion and Optoelectronic Materials, Technical Institute of Physics and Chemistry (TIPC), Chinese Academy of Sciences, Zhongguancun Beiyitiao 2, Haidianqu, Beijing 100190, China

[‡]Graduate University of Chinese Academy of Sciences, Beijing 100864, China

Supporting Information

ABSTRACT: A simple, mild, and effective self-templated etching strategy has been developed to directly convert SiO_2 nanospheres into surface-rough SiO_2 (SR-SiO_2) nanoparticles (NPs) by reaction with $NaBH_4$. Small SiO_2 NPs on the surface of SR-SiO_2 NPs can be tailored by carefully regulating the reaction time. SiO_2 nanospheres with varied sizes were etched under varied reaction conditions. Subsequently, particulate coatings were constructed on slide glass using SR-SiO_2 NPs as building blocks through the Layer-by-Layer assembly. Slide glasses just coated with two cycles of SR-SiO_2 NPs followed by calcination and hydrophobic modification exhibited superhydrophobicity because of their dual-size surface roughness.

KEYWORDS: self-templated etching approach, surface-rough SiO_2 nanoparticles, Layer-by-Layer assembly, coatings, superhydrophobicity

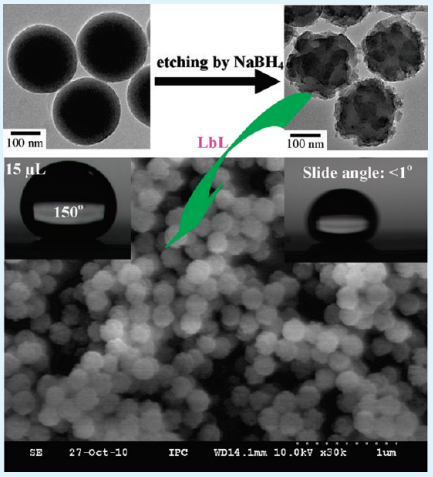

1. INTRODUCTION

Design and preparation of surface-rough (e.g., raspberry-like) nanoparticles (NPs) have attracted much attention because of their special structure and wide applications in catalysts, sensing, and especially in constructing superhydrophobic coatings (films) by mimicking the lotus leaf surface structure with dual-size roughness.[1,2] Superhydrophobicity of solid surfaces is an attractive topic in material science for its scientific significance and numerous potential applications, such as self-cleaning glass,[5−7] anti-icing on glass surfaces,[3,4] prevention of snow adhesion to glass, anticorrosion, anti-biofouling, and so on.

Recently, there have been a few reports focused on the fabrication of superhydrophobic surfaces with dual-size hierarchical structures originating from surface-rough particles.[8−11] Ming et al. prepared a superhydrophobic film with dual-size surface roughness by synthesizing silica-based raspberry-like particles and depositing them on an epoxy-based polymer film.[8] A complex procedure was, however, required to prepare the raspberry-like particles, including the preparation of amino-functionalized NPs and epoxy-functionalized microparticles, a reaction between the nano- and microparticles, and a long reaction and separation process. Zhang et al. prepared raspberry-like particles by assembling nano-sized SiO_2 particles on the surface of poly(acrylic acid)-functionalized polystyrene (PS) particles during the hydrolysis process.[9] Our previous works also reported the fabrication of raspberry-like NPs by in situ formation of nano-sized SiO_2 particles on the surface of O_2-plasma treated PS particles and by Layer-by-Layer (LbL) assembly of small-sized SiO_2 particles on the surface of large-sized SiO_2 particles or PS particles, respectively.[13−15] The latter two methods are also relatively complex and time consuming. Very recently, Yin's group reported several simple, mild, and effective surface-protected etching strategies to directly convert solid SiO_2 nanospheres into hollow or porous or rattle-type structures.[16−20] However, the formation of surface-rough SiO_2 (SR-SiO_2) NPs in the initial stage of etching was neglected in their work.[16]

In the current work, we investigated the fabrication of SR-SiO_2 NPs by the self-templated etching strategy. Solid SiO_2 nanospheres were directly converted into SR-SiO_2 NPs by reacting with $NaBH_4$. Compared with the above-mentioned methods, the current method has several advantages. First, it is very simple and is a one-step process that directly converts solid SiO_2 spheres into SR-SiO_2 NPs. Second, the procedure does not require high temperature or high pressure. Third, final SR-SiO_2 NPs are very

Received: January 21, 2011
Accepted: March 7, 2011
Published: March 17, 2011

ACS Publications © 2011 American Chemical Society

uniform in morphology and structure. Particulate coatings were constructed on slide glasses using SR-SiO_2 NPs as building blocks through the LbL assembly. After calcination and hydrophobic modification, the fabricated coatings exhibited the superhydrophobic property because of their dual-size surface roughness and low surface energy.

2. EXPERIMENTAL SECTION

2.1. Materials. Aqueous ammonia (25−28%), ethanol, sodium borohydride ($NaBH_4$, 97%), concentrated sulfuric acid (98%), and hydrogen peroxide (30%) were purchased from Beijing Chemical Reagent Company. Sodium poly(4-styrenesulfonate) (PSS, M_w = about 70,000), tetraethoxysilane (TEOS) (≥98%), and 1H, 1H, 2H, 2H-perfluorooctyltriethoxysilane (POTS, 97%; boiling point, 95 °C) were obtained from Alfa Aesar. Poly(diallyldimethylammonium chloride) (PDDA, M_w = 200,000−350,000, 20 wt %) was purchased from Aldrich. Polyvinylpyrrolidone ($[-CH_2CH(NCH_2CH_2CH_2CO)-]_n$, PVP, K-30, M_w = about 10000−70000) was purchased from Xilong Chemical Plant (Shantou, Guangdong). All chemicals were analytic grade and used without further purification. Ultrapure water with a resistivity higher than 18.2 MΩ cm was used in all experiments and was obtained from a three-stage Millipore Mill-Q Plus 185 purification system (Academic).

2.2. Synthesis of Monodisperse SiO_2 Nanospheres. Monodisperse SiO_2 nanospheres with varied sizes were prepared using a slightly modified Stöber process. In a typical synthesis of 240 nm SiO_2 nanospheres, 8 mL of water, 5 mL of ammonia solution, and 100 mL of ethanol were mixed. After the mixture was vigorously stirred for 30 min at 50 °C to form a homogeneous solution, 5 mL of TEOS was quickly added. The resulting mixture was again vigorously stirred at 50 °C for 6 h. The resulting precipitate was obtained by repeated washing/centrifugation/redispersing. By fixing the concentrations of TEOS and H_2O, but varying the added volume (3.5 and 12 mL, respectively) of ammonia solution, SiO_2 nanospheres of 140 and 350 nm in size were readily obtained, respectively.

2.3. Synthesis of SiO_2 NPs with Rough Surface. SiO_2 NPs with rough surface were obtained through the reaction between SiO_2 nanospheres with $NaBH_4$.[16,18] In a typical process, about 0.3 g of SiO_2 nanospheres and 0.25 g of PVP were first dispersed in 10 mL of water. After the mixture was treated by ulrasonication (100 w) for 10 min and stirred for 1 h, 0.6 g of $NaBH_4$ was added to the solution under vigorous stirring, followed by stirring for 30 min at room temperature. Then the mixture was stirred at 50 °C for 5 h. The resulting precipitate was obtained, centrifuged, washed with pure water and ethanol, and finally redispersed in pure water.

2.4. Preparation of Particulate Coatings with Dual-Size Roughness. Particulate coatings with dual-size roughness were fabricated on slide glasses using SR-SiO_2 NPs of about 220 nm as building blocks by the LbL assembly. The procedure is divided into three steps and described as follows.[5−7] First, commercially available glass or silicon substrates were cleaned with Pirhana solution (98 wt %H_2SO_4/30 wt % H_2O_2, 7/3, v/v) and then washed with pure water (Caution: The Pirhana solution is highly dangerous and must be used with great care). The cleaned substrates were alternately dipped in a PDDA and a PSS solution for 5 min, and redundant polyelectrolytes were removed by shaking in pure water for 2 min and rinsing for 1 min, followed by drying with N_2 flow at room temperature. The concentrations of PDDA and PSS aqueous solutions were 2 mg mL^{-1}. Mutilayers of $(PDDA/PSS)_5$/PDDA were prepared and were used as a primer in all experiments. Second, the $(PDDA/PSS)_5$/PDDA covered substrates were alternately dipped in an aqueous suspension of SR-SiO_2 NPs (0.5 wt %) and a PDDA solution (2 mg mL^{-1}) by the same procedure for an appropriate number of cycles. Finally, the as-prepared coatings were calcined (heating rate: 1 K min^{-1}) at 550 °C for 3 h to remove the polyelectrolytes.

2.5. Hydrophobic Modification of Particulate Coatings with Dual-Size Roughness. Hydrophobic modification of the fabricated particulate coatings on slide glasses was carried out by a simple chemical vapor deposition (CVD) of POTS.[5−7] The slide glasses with particulate coatings were placed in a Teflon container and sealed by stainless steel autoclave, on the bottom of which was dispensed a few droplets (10−20 μL) of POTS. There was no direct contact between the substrate and the POTS droplets. The autoclave was put in an oven at 120 °C for 2 h to enable the vapor of POTS to modify the coating surface. Finally, the autoclave was opened and placed in oven at 150 °C for an additional 1.5 h to volatilize unreacted POTS molecules on the coating.

2.6. Characterization. Scanning electron microscopy (SEM) observations were carried out on a Hitachi S-4300 field emission scanning electron microscope operated at 10 kV. Powder products were dispersed in ethanol by sonication for 10 min. They were then dropped onto the surface of silicon wafer and dried at 60 °C overnight. The specimens were coated with a layer of gold by ion sputtering before SEM observations. For transmission electron microscopy (TEM) observations, the powder products were dispersed in ethanol by sonication for 10 min and added on carbon-coated copper grids. After drying at 60 °C overnight, they were observed on a JEOL JEM-2100F transmission electron microscope at an acceleration voltage of 150 kV. Fourier transform infrared (FTIR) spectra were collected on an Excalibur 3100 FTIR spectrometer. The surface morphologies of SiO_2 particulate coatings were investigated by atomic force microscopy (AFM) on a Nanoscope IIIa AFM microscope under ambient conditions. AFM was operated in the tapping mode with an optical readout using Si cantilevers. Fourier transform infrared (FTIR) spectra were recorded on a Varian Excalibur 3100 spectrometer. Water contact angles (WCAs) of coating surfaces were measured at ambient temperature on a JC2000C contact angle/interface system (Shanghai Zhongchen Digital Technique Apparatus Co.). The values of WCAs were given by hypsometry (not goniometry), and the angle precision of which is ±0.5°. Water droplets of 15 μL were dropped carefully onto the coating surfaces. Once a water droplet contacted the sample surface, the machine began to take photos at a speed of 30 photos/s, i.e., the interval between the contact moment and the first image was 33 ms. The measurement was carried out on three different areas of the sample surface.

3. RESULTS AND DISCUSSION

Synthesis of SiO_2 NPs with Rough Surface by Reaction with $NaBH_4$. The added $NaBH_4$ amount in the starting suspension has a great effect on the morphology and structure of final particles. Figure S1 of the Supporting Information shows the morphology and structure of fabricated monodisperse SiO_2 nanospheres with a diameter of about 140 (a,b), 240 (c,d) and 350 nm (e,f), respectively. Taking SiO_2 nanospheres of 240 nm as example, varied amounts of $NaBH_4$ in 10 mL of water were applied, while fixing the reaction time at 5 h. When the added $NaBH_4$ amount is 0.4 g, SiO_2 nanospheres do not exhibit significant changes in morphology and structure except for a slightly decreased diameter (about 220 nm) due to etching under basic conditions (Figure 1a). When the added $NaBH_4$ amount increases to 0.6 g, SR-SiO_2 NPs with a diameter of about 220 nm are obtained (Figure 1b). The size of small NPs protruding on the surface of SR-SiO_2 NPs is about 20−80 nm. When the added $NaBH_4$ amount further increases to 0.8 g, core−shell particles of 200 nm in diameter form, which have a core of 100 nm in diameter and a shell of 50 nm in thickness. It is noted that some

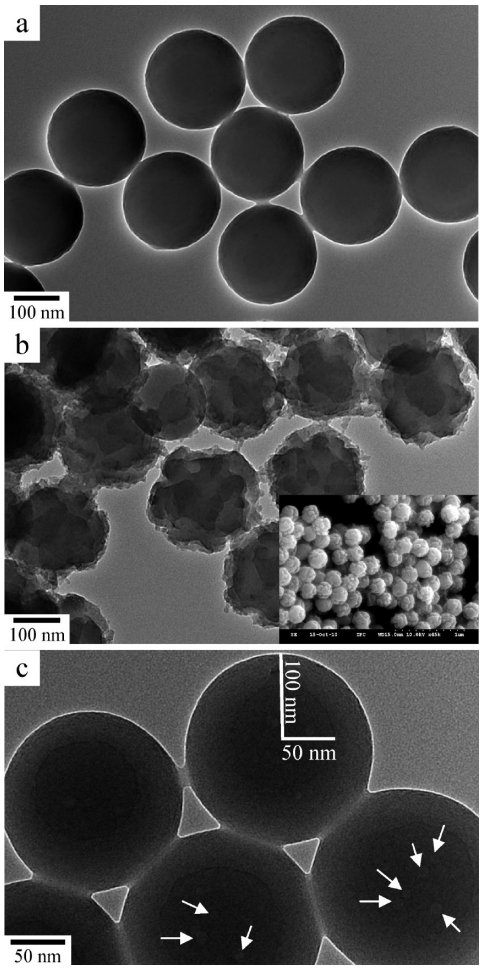

Figure 1. TEM images of products obtained by etching SiO_2 nanospheres of 240 nm using 0.4 g (a), 0.6 g (b), and 0.8 g (c) of $NaBH_4$, respectively, in 10 mL of water for 5 h.

small cavities of about 10 nm appear in the core (pointed by white arrows). Thus, the core−shell particles may be an intermediate product from solid spheres to hollow spheres. When the added $NaBH_4$ amount increases to 1.2 g, the product becomes bulk solid (the SEM image was not given), indicating that dissolved silicate species condense into bulk solid after the complete dissolution of SiO_2 nanospheres.

Because of the formation of SR-SiO_2 NPs by applying 0.6 g of $NaBH_4$, it would be expected that the surface roughness of SR-SiO_2 NPs could be tailored by regulating the reaction time. When the reaction time is 2 h, SiO_2 NPs with a slightly decreased diameter of about 220 nm and smooth surface are obtained (Figure S2 of the Supporting Information). When the reaction time increases to 3 h, small SiO_2 NPs of 10−20 nm form on the surface of SiO_2 NPs with a diameter of about 220 nm (Figure 2a), and when the reaction time increases to 4 h, small SiO_2 NPs of 20−60 nm appear on the surface of SiO_2 NPs with a diameter of about 220 nm (Figure 2b). Thus, the size of small SiO_2 NPs on the surface of SR-SiO_2 NPs can be readily adjusted by carefully tailoring the reaction time, and when the reaction time increases to 10 h, fractured and aggregated hollow SiO_2 NPs of about 200 nm in size form (Figure S3 of the Supporting Information). The size of hollow cavity is about 60−120 nm.

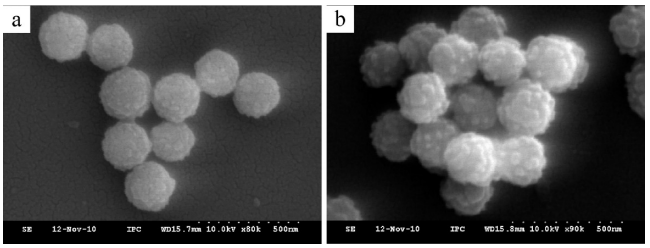

Figure 2. SEM images of products obtained by etching SiO_2 nanospheres of 240 nm for 3 h (a) and 4 h (b), using 0.6 g of $NaBH_4$ in 10 mL of H_2O, respectively.

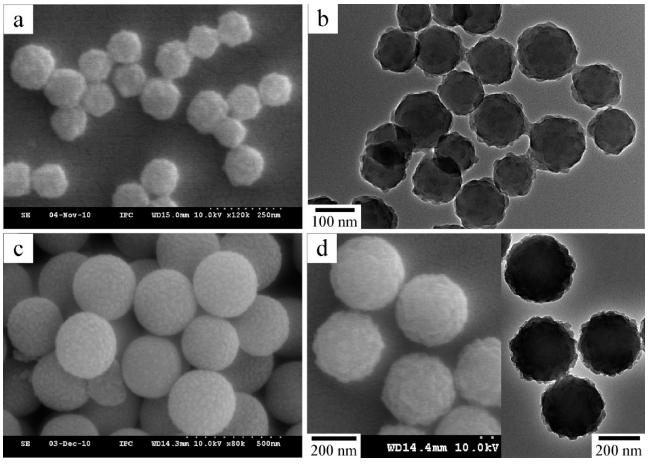

Figure 3. SEM and TEM images of products obtained by etching SiO_2 nanospheres of 140 nm (a,b) for 4 h using 0.6 g of $NaBH_4$ in 10 mL of water and by etching SiO_2 nanospheres of 350 nm for 3 h (c) and 5 h (d) using 0.6 g of $NaBH_4$ in 10 mL of water, respectively.

SiO_2 nanospheres of about 140 nm were also tried as a self-template to fabricate SR-SiO_2 NPs by reaction with 0.6 g of $NaBH_4$ for 4 h. Panels (a) and (b) of Figure 3 show the fabricated SR-SiO_2 NPs with a diameter of about 130 nm after etching SiO_2 nanospheres of about 140. The size of small SiO_2 NPs protruding on the surface of etched particles is about 10−30 nm. SiO_2 nanospheres of about 350 nm were also used as a self-template to fabricate SR-SiO_2 NPs by reaction with 0.6 g of $NaBH_4$ for 3 and 5 h, respectively. For 3 h etching, small SiO_2 NPs of 10−30 nm homogeneously cover on the surface of SR-SiO_2 NPs with a diameter of 330−340 nm (Figure 3 c). After etching for 5 h, SR-SiO_2 NPs with a diameter of about 320 nm were obtained, and the size of small SiO_2 NPs on the surface of etched particles is about 10−40 nm (Figure 3 d).

Figure 4 shows FTIR spectra of the SiO_2 materials. Curve (1) is the FTIR spectrum of as-prepared SiO_2 nanospheres (diameter: 240 nm). A broad band with a maximum about 3431 cm^{-1} is attributed to the O−H stretching in both Si−OH groups and some physisorbed water, which is also confirmed by the presence of H_2O deformation band (the bending vibration of H−O−H groups) at ca. 1638 cm^{-1}. Weak absorption bands attributed to C−H bending vibration in unhydrolyzed $-OC_2H_5$ groups are observed at near 1398 cm^{-1}. Bands located at 1103, 953, and 801 cm^{-1} are associated with the Si−O−Si asymmetric bond stretching vibration, the Si−OH stretching vibration, and the network Si−O−Si symmetric bond stretching vibration,

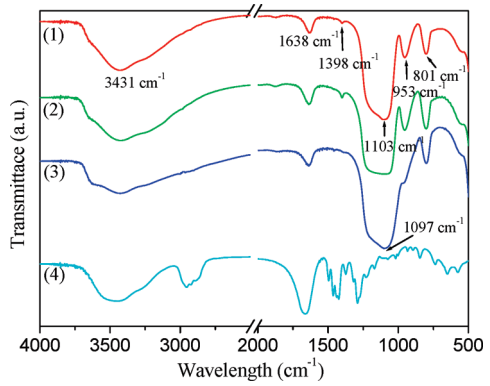

Figure 4. FTIR spectra of as-prepared SiO_2 nanospheres (diameter: 240 nm) (1), SiO_2 nanospheres treated by ultrasonication (100 W) for 10 min, stirred for 1 h, and washed with a little water (about 5 mL) (2), etched SiO_2 NPs (shown in Figure 1b) (3), and PVP (4).

respectively. After the suspension of PVP, SiO_2 nanospheres were treated by ultrasonication (100 W) for 10 min and stirred for 1 h. A total of 2 mL of the suspension was taken out, centrifuged, and washed once with about 5 mL of water, and the precipitate was dried at 60 °C. Curve (2) shows the FTIR spectrum of the precipitate. Compared with curve (4), which is the FTIR spectrum of PVP, no characteristic PVP absorption peaks are observed, indicating no PVP adsorption on the surface of SiO_2 nanospheres. Curve (3) exhibits the FTIR spectrum of etched SiO_2 particles (Figure 1b), which had been dried at 60 °C. The intensity of the bands related to the C−H bending vibration becomes indistinguishable, indicating that the residual $-OC_2H_5$ groups had been completely hydrolyzed during the reaction. The Si−O−Si asymmetric stretching vibration band shows a ~6 cm^{-1} red shift from 1103 to 1097 cm^{-1} during the conversion from the solid to the surface-rough particles. It is much smaller than the red shift (~23 cm^{-1}) during the solid-to-hollow conversion observed by Zhang et al.,[16] indicating that the surface-rough particles have a denser network structure than that of hollow particles.[16,21] The Si−OH stretching vibration band at 953 cm^{-1} cannot be easily discerned because of its overlap with the red-shifted Si−O−Si asymmetric stretching vibration band.

Etching Mechanism. A mechanism was previously proposed in the literature for the solid-to-hollow transformation under similar conditions, which consists of two separate processes: the dissolution of SiO_2 and the regrowth of the silica layer.[16,18] The current experimental results unveiled the unobserved period of morphology evolution under similar conditions, which could supplement and further support the proposed mechanism. Thus, on the basis of the structure evolvement of the etched SiO_2 NPs with an increase in time and the previously proposed mechanism, a plausible etching process is depicted in Scheme 1.[16−20] After the addition of $NaBH_4$, $NaBH_4$ reacts with water to slowly release H_2 and sodium metaborate ($NaBO_2$) ($NaBH_4 + 2H_2O \rightarrow 4H_2\uparrow + NaBO_2$). After stirring for 1 h, the pH value of suspension is 10.02 because $NaBO_2$ is a strong base ($BO_2^{-1} + H_2O \rightarrow HBO_2 + OH^{-1}$). At 50 °C, the slow dissolution of SiO_2 ($2OH^{-1} + SiO_2 \rightarrow SiO_3^{2-} + H_2O$) will occur due to the high basicity and the weak protection role of PVP (low adsorbed amount), which can dissociate Si−O bonds and form soluble monosilicate and polysilicate species with various compositions, thus leading to the shrinkage in size of the amorphous SiO_2 nanospheres (Figure S2 of the Supporting Information and Scheme 1b). With an increase in reaction time, the silicate species eventually becomes supersaturated along with the dissolution of silica, and the concentration of BO_2^{-1} and OH^{-1} increases gradually as a result of the decomposition of $NaBH_4$. Then, small SiO_2 NPs (10−20 nm) appear on the surface of SiO_2 nanospheres due to the redeposition of silicate species on the surface of SiO_2 nanospheres (Figure 2a and Scheme 1c). Small SiO_2 NPs further grow (from 10−20 nm to 20−60 nm to 20−80 nm, Figures 2b and 1b, and Scheme 1d,e) at the expense of the cores through a mechanism similar to Ostwald ripening, eventually leading to the production of completely hollow SiO_2 NPs (Figure S3 of the Supporting Information and Scheme 1f).[16] It is interesting that the redeposited small SiO_2 NPs can withstand etching in the strong basic condition. The reason may be that the redeposited SiO_2 species may have a denser network structure (higher condensation degree) than that of the core SiO_2 species. In fact, previous studies on SiO_2 colloid synthesis indicated that SiO_2 NPs are formed by the aggregation of nuclei, followed by further growth.[22] Thus, the internal parts of the silica particles are presumably less dense and more porous,[23] resulting in the preferential dissolution of core SiO_2. After reacting for 5 and 10 h at 50 °C, the pH value of the suspension reaches to 10.96 and 11.12, respectively. The increase in pH from 10.02 to 10.96 to 11.12 may affect the rate of etching, thus playing an important role in the formation of NPs with varied morphologies and structures.

Scheme 1. Schematic illustration of the morphologies and structures of products obtained at varied reactive times: (a) 0 h, (b) 2 h, (c) 3 h, (d) 4 h, (e) 5 h, and (f) 10 h

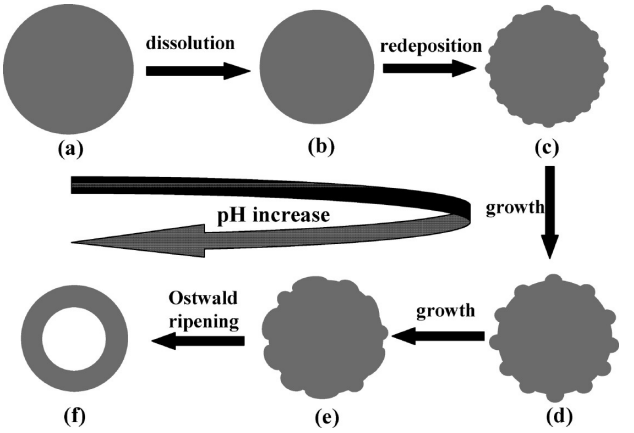

It is worth noting that recently Part et al. have also reported a size-dependent shape evolution of solid SiO_2 NPs into hollow structures under slightly basic conditions as a result of base-catalyzed etching.[24] The conversion process is that small pores are formed inside the NPs, which are merged into a large cavity, generating hollow structures. The internal parts of the SiO_2 NPs are preferentially etched because SiO_2 NPs with small sizes have the more porous and less dense structure than those with large sizes. The two hollowing processes might involve similar chemical reactions, but the shape transformation pathways appear to be distinct.

Construction of Particulate Coatings with Dual-Size Roughness. The rough surface morphology of the fabricated SR-SiO_2 NPs makes them ideal building blocks for the fabrication of superhydrophobic coatings. Taking SR-SiO_2 NPs (shown

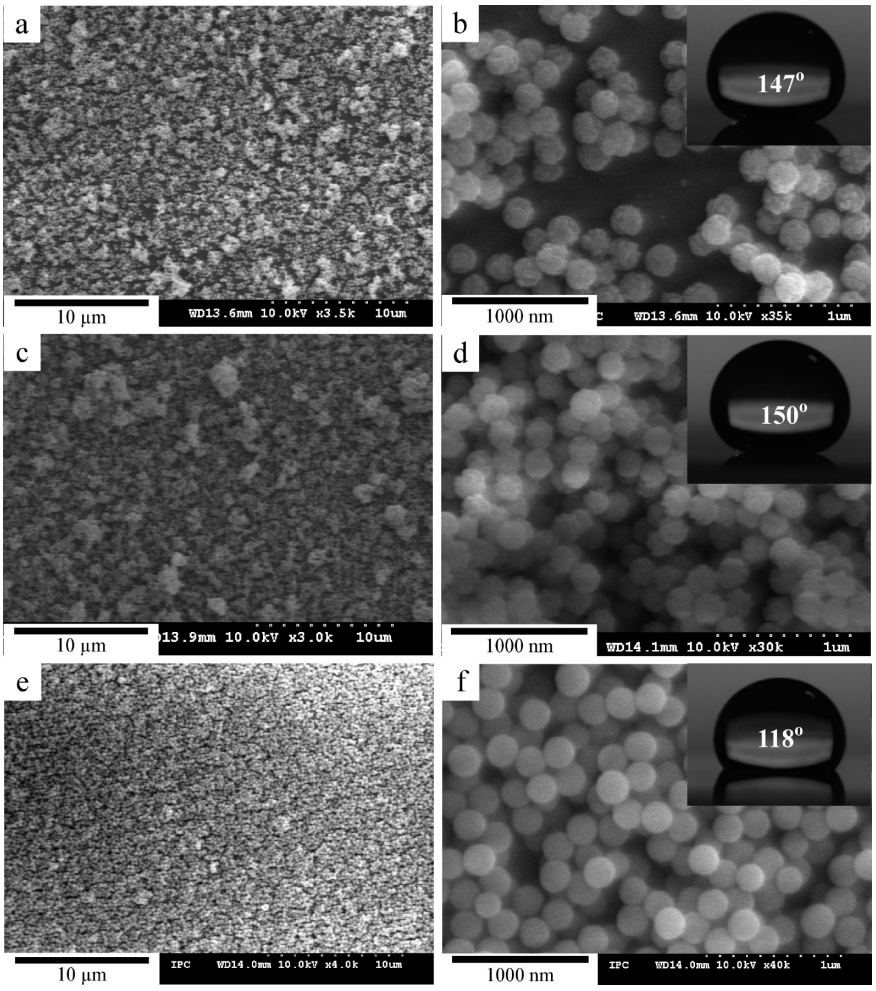

Figure 5. SEM images of particulate coatings on slide glasses by alternate LbL deposition of PDDA/SR-SiO_2 of two cycles (a,b) and four cycles (c,d), and of PDDA/SiO_2 of four cycles (e,f) followed by calcination and hydrophobic modification. The insets are images of corresponding static water contact angles measured using contact-mode; the volume of water droplets is 15 μL.

in Figure 1b) as typical example, they are about 220 nm in diameter and small NPs on their surface are about 20−80 nm in size. Particulate coatings were constructed on slide glasses through the LbL assembly.

Polycation (PDDA) and polyanion (PSS) can be readily adsorbed on the surface of Piranha solution-treated slide glasses. As a result, a thin film of desired surface charges can be obtained on the surface of slide glasses. There are many silanol groups on the surface of SR-SiO_2 NPs (curve (3) in Figure 4), and the point of zero charge is 2.1 for SiO_2 (the pH value of SiO_2 suspension is about 9),[25] which renders the surface of SR-SiO_2 NPs slightly negatively charged in aqueous solution. Thus, SR-SiO_2 NPs can be adsorbed alternately with PDDA on the surface of the slide glass with a primer. To attain a desired particulate density on the surface of the slide glass, a varied number of PDDA/(SR-SiO_2 NPs) cycles were deposited. The attractive long-range van der Waals forces, the repulsive electrostatic interaction between the like-charge SR-SiO_2 NPs plus the attractive electrostatic interaction between SR-SiO_2 NPs and the PDDA layer, are the critical terms governing the adsorption processes.

SEM images in Figure 5 show surface morphologies of particulate coatings with PDDA/SR-SiO_2 of two cycles (Figures 5a, b) and four cycles (Figures 5c,d) followed by calcination and hydrophobic modification. Clearly, SR-SiO_2 NPs are homogenously scattered on the substrate surface. Magnified SEM images (Figures 5b,d) reveal that the coating surface in fact consists of nanometer-sized islands (composed of SR-SiO_2 NPs) and valleys (voids among SR-SiO_2 NPs). By comparing panels (b) and (d) of Figure 5, it is shown that the particle density, coating thickness, and surface roughness increase gradually and significantly by increasing the number of deposition cycles. For comparison, SiO_2 nanospheres with a diameter of 240 nm were also used to fabricate a particulate coating with PDDA/SiO_2 of four cycles, and the surface morphology is shown in panels (e) and (f) of Figure 5. Compared with panels (d) and (f) of Figures 5, the particulate densities on the glass slides are nearly the same, indicating that the surface roughness difference of particles has no significant influence on the amount of NPs adsorbed in the LbL process. AFM was used to measure the degree of surface roughness of coatings. The root-mean-square (rms) roughness of the particulate coatings deposited with two and four cycles of PDDA/SR-SiO_2 and four cycles of PDDA/SiO_2 followed by calcination and hydrophobic modification is 111, 130, and 66 nm, respectively. Clearly, the particulate coatings composed of SR-SiO_2 NPs are much rougher on surface than those of SiO_2 nanospheres. Such morphologies of high surface roughness

might significantly influence the wetting property of the coatings.[9−15]

FTIR spectroscopy was used to characterize the surface groups of particulate coatings. Figure 6 shows the FTIR spectrum of etched SiO_2 NPs (Figure 1b) after calcination (550 °C, 3 h) (cal-etched SiO_2 NPs). Compared with the FTIR spectrum of etched SiO_2 NPs (curve (3) in Figure 4), the absorption peaks of Si−OH and H_2O around 3431 and 1638 cm^{-1} significantly decrease, the absorption peak of the Si−OH stretching vibration around 953 cm^{-1} disappears, and the absorption peak of the Si−O−Si asymmetric bond stretching vibration has a blue shift from 1097 to 1111 cm^{-1}, indicating that the calcination causes disappearance of Si−OH groups, significant reduction of physisorbed water, and formation of a denser network structure. After cal-etched SiO_2 NPs were modified by POTS molecules (POTS-cal-etched SiO_2 NPs), FTIR spectrum of POTS-cal-etched SiO_2 NPs shows some new absorption peaks (indicated by black arrows) compared with those of cal-etched SiO_2 NPs. Compared with the FTIR spectrum of POTS, the appearance of new absorption peaks proves the existence of POTS species (not POTS molecules because the heating at 150 °C excludes the possible existence of POTS molecules (POTS boiling point: 95 °C)), thus indicating the successful modification of coatings by POTS. The newly appeared absorption peaks are so small that they are difficult to observe, indicating that the amount of POTS species is very small, and there may just exist a single layer of POTS species on the surface of cal-etched SiO_2 NPs. Because of the very few Si−OH groups on the surface of cal-etched SiO_2 NPs, the achievement of the successful modification should have resulted from the hydrolysis and condensation reaction between POTS molecules and physisorbed H_2O molecules (and the very few Si−OH groups) on the surface of cal-etched SiO_2 NPs. Then we examined the effect of Si−OH on POTS modification. After calcination (550 °C, 5 h), FTIR spectrum (Figure S4 of the Supporting Information) of conventional MCM-41 NPs (diameter: about 100 nm) still shows the absorption peak of the Si−OH stretching vibration around 958 cm^{-1} (indicated by dot line) due to their high specific surface area (about 1000 $m^2 g^{-1}$), indicating the existence of Si−OH groups. The absorption peaks around 3431 and 1638 cm^{-1} from Si−OH and H_2O also exist because of incomplete removal of Si−OH and physisorbed H_2O molecules. After POTS medication, newly appeared absorption peaks (indicated by black arrows) are also very small, again indicating that the amount of modifing POTS species is very small. Thus, it can be concluded that the existence of Si−OH groups cannot significantly increase the amount of modifing POTS species. The following tests of wettability indicate that the existence of a small amount of POTS species can significantly increase the water contact angle.

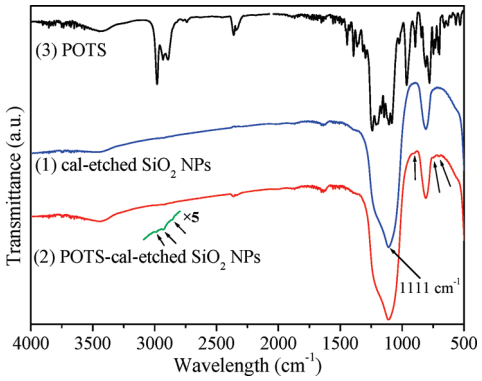

Figure 6. FTIR spectra of etched SiO_2 NPs after calcination (550 °C, 3 h) (1), etched SiO_2 NPs after calcination and POTS modification (2), and POTS (3).

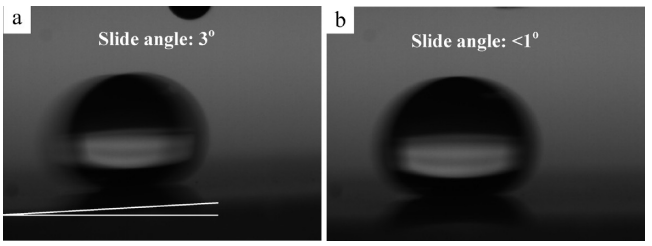

Figure 7. Digital images of sliding angles on particulate coatings assembled by alternate LbL deposition of PDDA/SR-SiO_2 of two cycles (a) and four cycles (b) followed by calcination and hydrophobic modification. The volume of water droplets is 15 μL.

It is known that the wettability of a solid surface is controlled both by its surface energy, which is determined by its components and by its surface roughness or porosity. Early theoretical works by Wenzel,[26] Cassie−Baxter,[27] and Quéré[28] and more recent studies[29−32] indicated that the construction of hierarchical micro- and nanostructures with high surface roughness and porosity is an effective approach to tailor the wettability of a surface. In the current work, when the volume of water droplet is 3 μL, water contact angles (WCAs) after 1 s of spreading on the particulate coatings composed of PDDA/SR-SiO_2 of two cycles (a) and four cycles (b), and of PDDA/SiO_2 of four cycles (c) followed by calcination are about 5.2, 4.8, and 6.5°, respectively (Figure S5 of the Supporting Information). These results are in agreement with the surface roughnesses of corresponding coatings.

After hydrophobic modification by POTS, the particulate coatings demonstrated superhydrophobicity. The contact-mode (Figure S6 of the Supporting Information) and drip-mode (Figure S7 of the Supporting Information) were chosen to measure WCAs on the coatings after hydrophobic modification, respectively.[6] The volumes of water droplets for the measurements were slightly smaller than 15 μL for the contact-mode and 15 μL for the drip-mode, respectively. In fact, water droplets with a volume of about 1−14 μL could not be dropped freely using a microsyringe because of the large capillary force between the

Table 1. WCAs on the Surface of Coatings after Hydrophobic Modification

particle type	cycle numbers	rms roughness[a]	static angle (deg)	advancing angle (deg)	receding angle (deg)	CA hysteresis (deg)	sliding angle (deg)
SiO_2	4	66	118 ± 1	–	–	–	>30
SR-SiO_2	2	110	147 ± 1	150 ± 1	144 ± 1	6 ± 2	3
SR-SiO_2	4	130	150 ± 1	153 ± 1	150 ± 1	3 ± 2	<1

[a] Obtained by AFM measurements.

water droplet and the tube of microsyringe, while 15 μL is the sole standard volume supplied by the peristaltic pump of our contact angle/interface system. We chose at least three different locations on the coatings, and there were very little difference in the WCAs measured at these locations, indicating the uniformity of the coating surfaces. When water droplets of slightly smaller than 15 μL were used in the contact-mode (Figure S6 of the Supporting Information), the substrate with the coating was raised to touch and slightly press the droplet in order to increase the adhesive force between the highly hydrophobic coating and the water droplet so that the water droplet can adhere on the coating surface (Figure S6 of the Supporting Information). The static WCAs on the surface of the slide glasses coated with two and four cycles of PDDA/SR-SiO_2 are 147° and 150°, respectively (inset in Figure 5b,d), which are significantly larger than that (118°) on the surface of slide glass coated with four cycles of PDDA/SiO_2. The sliding angles on the surface of the slide glasses coated with two and four cycles of PDDA/SR-SiO_2 are about 3° and <1°, respectively (Figure S8 of the Supporting Information, Figure 7, Table 1), which means water droplets could roll off these surfaces easily. In contrast, water droplets on the surface of slide glass coated with four cycles of PDDA/SiO_2 can not slide even the tilt angle of the apparatus is >30°. The larger the volume of water droplet is, the smaller the WCA is.[6,33] Thus, when water droplets of <15 μL (common 3 μL for example) are used, the WCAs must be larger than 147° for the coating of two cycles and larger than 150° for the coating of four cycles. Therefore, it can be concluded that the slide glass just coated with two cycles of SR-SiO_2 NPs already have superhydrophobicity.

In the drip mode, the water droplet of 15 μL could roll off the slide glasses coated with two and four cycles of PDDA/SR-SiO_2 easily and quickly, which may result from the kinetic energy of water droplet (Figure S7 of the Supporting Information).[6] When a water droplet drops from the tube of microsyinge down to the coating, it would have a momentum of 2.6×10^{-6} kg m s^{-1} and a kinetic energy of 2.2×10^{-7} J, which were estimated roughly from panel (a) of Figure S7 of the Supporting Information on the assumption of spheroid water droplet. Thus, a water droplet with momentum and kinetic energy was able to overcome the adhesive force between the coating and droplet water and rolled off the coating easily and quickly. During the sliding process, a water droplet may have not penetrated into the voids and pores of the coating. Thus, a water droplet could roll off the coating easily and quickly.

4. CONCLUSIONS

In summary, we have developed a facile self-templated etching route to the fabrication of SR-SiO_2 NPs by reaction between SiO_2 nanospheres and $NaBH_4$. The size of small SiO_2 NPs on the surface of SR-SiO_2 NPs can be tailored by carefully regulating the reaction time. SR-SiO_2 NPs with a diameter of about 240 nm were chosen as typical samples and building blocks to construct particulate coatings on slide glasses by the LbL assembly. Slide glass just coated with two cycles of SR-SiO_2 NPs followed by calcination and hydrophobic modification have superhydrophobicity because of its dual-size surface roughness. These SR-SiO_2 NPs may be promising in practical applications as building blocks to construct superhydrophobic coatings because of their facile and inexpensive fabrication.

■ ASSOCIATED CONTENT

Supporting Information. Additional SEM images of SiO_2 nanospheres with varied sizes, SEM and TEM images of SiO_2 hollow spheres obtained by etching, and digital images of water contact angles and sliding angles on the surface of coatings. This material is available free of charge via the Internet at http://pubs.acs.org.

■ AUTHOR INFORMATION

Corresponding Author
*Tel.: +86-10-82543535; Fax: +86-10-82543535; E-mail: jhhe@mail.ipc.ac.cn.

■ ACKNOWLEDGMENT

This work was supported by the Knowledge Innovation Program of the Chinese Academy of Sciences (CAS) (Grants KGCX2-YW-370, KGCX2-YW-111-5), the National Natural Science Foundation of China-NSAF (Grant 10776034), the National Natural Science Foundation of China (Grant 20871118), "Hundred Talents Program" of CAS, and "Graduate Science and Social Practice Special Funding Innovative Research Program" of CAS.

■ REFERENCES

(1) Feng, L.; Li, S.; Li, Y.; Li, H.; Zhang, L.; Zhai, J.; Song, Y.; Liu, B.; Jiang, L.; Zhu, D. *Adv. Mater.* **2002**, *14*, 1857–1861.
(2) Liu, K.; Yao, X.; Jiang, L. *Chem. Soc. Rev.* **2010**, *39*, 3240–3255.
(3) Cao, L.; Jones, A. K.; Sikka, V. K.; Wu, J.; Gao, D. *Langmuir* **2009**, *25*, 12444–12448.
(4) Mishchenko, L.; Hatton, B.; Bahadur, V.; Taylor, J. A.; Krupenkin, T.; Aizenberg, J. *ACS NANO*, DOI: 10.1021/nn102557p.
(5) Liu, X.; He, J. *J. Phys. Chem. C* **2009**, *113*, 148–152.
(6) Du, X.; Li, X.; He, J. *ACS Appl. Mater. Interfaces* **2010**, *2*, 2365–2372.
(7) Li, X.; Du, X.; He, J. *Langmuir* **2010**, *26*, 13528–13534.
(8) Ming, W.; Wu, D.; Van Benthem, R.; De With, G. *Nano Lett.* **2005**, *5*, 2298–2301.
(9) Qian, Z.; Zhang, Z.; Song, L.; Liu, H. *J. Mater. Chem.* **2009**, *19*, 1297–1304.
(10) Zhang, L.; Chen, H.; Sun, J.; Shen, J. *Chem. Mater.* **2007**, *19*, 948–953.
(11) Tsai, H.; Lee, Y. *Langmuir* **2007**, *23*, 12687–12692.
(12) Acunzi, M. D.; Mammen, L.; Singh, M.; Deng, X.; Roth, M.; Auernhammer, G. K.; Butt, H.; Vollmer, D. *Faraday Discuss.* **2010**, *146*, 35–48.
(13) Du, X.; Liu, X.; Chen, H.; He, J. *J. Phys. Chem. C* **2009**, *113*, 9063–9070.
(14) Liu, X.; Du, X.; He, J. *ChemPhysChem* **2008**, *9*, 305–309.
(15) Liu, X.; He, J. *J. Colloid Interface Sci.* **2007**, *314*, 341–345.
(16) Zhang, T.; Zhang, Q.; Ge, J.; Goebl, J.; Sun, M.; Yan, Y.; Liu, Y.; Chang, C.; Guo, J.; Yin, Y. *J. Phys. Chem. C* **2009**, *113*, 3168–3175.
(17) Zhang, Q.; Zhang, T.; Ge, J.; Yin, Y. *Nano Lett.* **2008**, *8*, 2867–2871.
(18) Zhang, T.; Ge, J.; Hu, Y.; Zhang, Q.; Aloni, S.; Yin, Y. *Angew. Chem., Int. Ed.* **2008**, *47*, 5806–5811.
(19) Zhang, Q.; Ge, J.; Goebl, J.; Hu, Y.; Lu, Z.; Yin, Y. *Nano Res.* **2009**, *2*, 583–591.
(20) Hu, Y.; Zhang, Q.; Geobl, J.; Zhang, T.; Yin, Y. *Phys. Chem. Chem. Phys.* **2010**, *12*, 11836–11842.
(21) Zhu, H.; Ma, Y.; Fan, Y. G.; Shen, J. C. *Thin Solid Films* **2001**, *397*, 95–101.
(22) Bogush, G. H.; Tracy, M. A.; Zukoshi, C. F. *J. Non-Cryst. Solids* **1988**, *104*, 95.

(23) Lecloux, A. J.; Bronckart, J.; Noville, F.; Dodet, C.; Marchot, P.; Pirard, J. P. *Colloids Surf.* **1986**, *19*, 359.
(24) Park, S. J.; Kim, Y. J.; Park, S. J. *Langmuir* **2008**, *24*, 12134–12137.
(25) Zhang, X. T.; Sato, O.; Taguchi, M.; Einaga, Y.; Murakami, T.; Fujishima, A. *Chem. Mater.* **2005**, *17*, 696–700.
(26) Wenzel, R. N. *Ind. Eng. Chem.* **1936**, *28*, 988–994.
(27) Cassie, A. B. D.; Baxter, S. *Trans. Faraday Soc.* **1944**, *40*, 546–551.
(28) Bico, J.; Thiele, U.; Quéré, D. *Colloid Surf. A* **2002**, *206*, 41–46.
(29) Hoshikawa, Y.; Yabe, H.; Nomura, A.; Yamaki, T.; Shimojima, T.; Okubo, T. *Chem. Mater.* **2010**, *22*, 12–14.
(30) Li, Y.; Liu, F.; Sun, J. *Chem. Commun.* **2009**, 2730–2732.
(31) Cebeci, F. Ç.; Wu, Z.; Zhai, L.; Cohen, R. E.; Rubner, M. F. *Langmuir* **2006**, *22*, 2856.
(32) Lee, D.; Rubner, M. F.; Cohen, R. E. *Nano Lett.* **2006**, *6*, 2305–2312.
(33) Yoshimitsu, Z.; Nakajima, A.; Watanabe, T.; Hashimoto, K. *Langmuir* **2002**, *18*, 5818–5822.